Medical Engineering & Physics xxx (2010) xxx–xxx

Contents lists available at ScienceDirect

Medical Engineering & Physics

journal homepage: www.elsevier.com/locate/medengphy

A fully automatic ocular artifact suppression from EEG data using higher order statistics: Improved performance by wavelet analysis

Hosna Ghandeharion, Abbas Erfanian*

Department of Biomedical Eng., Faculty of Electrical Eng., Iran Neural Technology Centre, Iran University of Science and Technology, Hengam Street, Narmak, 16844 Tehran, Iran

ARTICLE INFO

Article history:
Received 26 May 2009
Received in revised form 10 April 2010
Accepted 12 April 2010

Keywords:
Electroencephalogram
Ocular artifact
Independent component analysis
Wavelet analysis

ABSTRACT

Contamination of electroencephalographic (EEG) recordings with different kinds of artifacts is the main obstacle to the analysis of EEG data. Independent component analysis (ICA) is now a widely accepted tool for detection of artifacts in EEG data. One major challenge to artifact removal using ICA is the identification of the artifactual components. Although several strategies were proposed for automatically detecting the artifactual component during past several years, there is still little consensus on the criteria for automatic rejection of undesired components. In this paper we present a new identification procedure based on an efficient combination of independent component analysis (ICA), mutual information, and wavelet analysis for fully automatic ocular artifact suppression. The method does not require any offline training or determining the threshold levels for different markers. The results show that the proposed method could significantly enhance the ocular artifact detection and suppression. The results on 3105 4-s EEG epochs indicate that the artifact components can be identified with an accuracy of 97.8%, a sensitivity of 96.9%, and a specificity of 98.6%.

1. Introduction

Contamination of electroencephalographic (EEG) recordings with different kinds of artifacts such as eye movements and blinks is the main obstacle to the analysis of EEG data. These types of artifact may interfere with the detection and analysis of events of interest and hinder the interpretation of EEG recordings. The traditional method of the eye-blink suppression is the removal of the segment of EEG data in which eye blinks occur. Eye blinks are usually detected by means of data recorded from electrodes placed above and below the subject's eye. An eye blink is said to have occurred if the signal amplitude exceeds a given threshold. All EEG segments in which eye blinks occur are then excluded. In addition, in some event-related potential experiments, eye blinks superimpose on evoked-response components. In this case, a common approach is to reject all EEG epochs containing the signal amplitude larger than some selected value. These schemes are rigid and do not lend themselves to adaptation. Moreover, a portion of data will be lost.

Several methods based on regression in the time domain [1] or frequency domain [2] have been proposed for removing ocular artifacts. This approach estimates the influence of EOG on the signals recorded by scalp electrodes and removes it from the EEG recordings. However, regression methods require a good regression channel (e.g., EOG). Due to the bidirectional mixture of ocular and cerebral activities, regression methods inevitably involve subtracting relevant EEG data contained in the EOG channel(s) from the EEG channels.

The so-called blind source separation (BSS) techniques open a new approach to ocular artifact reduction. BSS methods are based on a linear decomposition of the EEG and EOG recordings into source components. These component-based methods segregate artifactual activities into separate sources, hence, the reconstruction of EEG recordings without these sources leads to artifact reduction. The first proposed component-based procedure was Principle Component Analysis (PCA) [3]. However, PCA cannot completely separate eye artifacts from EEG signals, especially when they have comparable amplitude [4–6]. Berg and Scherg [7] proposed a method based on the combination of PCA, multiple source models of EEG and EOG, and an artifact-aligned averaging method to correct eye artifacts. However, the accuracy of the method depends on availability of an accurate model of brain activity, head model and independent estimate of the spatial distribution of eye activity throughout the head.

To overcome the limitations and constraints of regression and PCA, a more effective component-based method has been introduced for removing a wide variety of artifacts from multichannel EEG recordings based on independent component analysis (ICA)

* Corresponding author at: Department of Biomedical Engineering, Iran University of Science and Technology, Iran Neural Technology Centre, Tehran, Iran. Tel.: +98 21 77240465; fax: +98 21 77240490.
E-mail address: erfanian@iust.ac.ir (A. Erfanian).

1350-4533/$ – see front matter © 2010 IPEM. Published by Elsevier Ltd. All rights reserved.
doi:10.1016/j.medengphy.2010.04.010

[5,6,8–13]. Jung et al. [8] showed that ICA can effectively detect, separate, and remove a wide variety of artifacts (including ocular artifacts, muscle artifacts, and line noise power) from contaminated EEG recordings.

The acquired results in [14] supported the use of regression-based and PCA-based ocular artifact correction and suggested a need for further studies examining possible spectral distortion from FastICA-based correction procedures [15]. Recently, Romero et al. [16] objectively and quantitatively evaluated the performance of varied ocular filtering methods. They applied regression and different BSS techniques to different montages of simulated EEG and EOG recordings and finally concluded the effectiveness of BSS-based algorithms for eye movement removal even when EOG recordings were not available or when data length was short. Delorme et al. [12] reported that ICA preprocessing led to a 10–20% increase in detection performance for all ICA algorithms tested.

Despite all the practically verified virtues of ICA, the method requires visual inspection of extracted components and manual classification of the interference components. This can be time-consuming and is not desirable for real-time artifact suppression. To overcome the shortcomings of the visual inspection approach, many automatic methods have been proposed and reported [16–25]. James and Gibson [17] used constrained ICA (cICA) to extract a single independent component (IC) that is constrained to be similar to some reference signal. The method was employed for eye-blink suppression in multichannel recordings of EEG and MEG. To obtain a reference signal, a simple threshold is applied to Fp1 and a positive going pulse is recorded when the EEG at Fp1 exceeds that threshold. Barbati et al. [18] used kurtosis and entropy of ICs and the correlation coefficients between the power spectrum density (PSD) of the estimated ICs and the PSD of EOG to automatically identify artifactual ICs in magnetoencephalographic signals.

Another procedure for automated correction of ocular artifacts in EEG records using blind source separation (BSS) and correlation metrics was proposed by Joyce et al. [19]. They used the correlation between the BSS components and vertical and horizontal EOG signals and the power of BSS components in the low frequency band to identify the eye-blink components. Moreover, BSS applied to the data with reversing the sign of vertical and horizontal EOG signals. Comparing the resulted components with those obtained by applying the BSS to the original data, the components that inverted were eliminated. In order to remove artifacts from magnetoencephalogram (MEG) background activity, Escudero et al. [25] used the power in the low frequency band of each IC to decide which ICs accounted for ocular artifacts. Li et al. [20] proposed the template matching method for selecting the eye-blink artifact component. They used a fixed pattern of the scalp topography as a template and selected the component whose scalp topography was most similar to the template under certain distance measure. However, this method requires obtaining the topographic template be obtained beforehand and the visual inspection of the topography of the ICs. The relative power spectrum and scalp topographies of the independent components were also used for automatic artifact identification [16]. An independent component (IC) was identified as artifactual component when the relative power in the delta frequency and the projection strength of the IC onto the EOG electrodes exceeded a predefined threshold and the projection strengths of the IC onto EEG electrodes have values higher than a threshold and follow a gradient depending on the artifact.

LeVan et al. [21] devised an ICA-based automated system to remove artifacts from ictal scalp EEG, using a Bayesian classifier. The classifier was trained using numerous statistical, spectral, and spatial features. Recently, Okada et al. [24] presented an ICA-based method for removing eye-blink artifacts in event-related MEG measurements. The similarity between normalized MEG measurements for five successive sampling points centered at EOG peak latency and the topographic pattern of each IC was used as a marker for identifying the artifactual components. The IC with the largest similarity was selected as the eye-blink component. The EOG peak latency was determined by searching the maximum EOG for the duration where EOG exceeded a certain threshold potential.

However, all these automated methods share an inherent weakness, in that they are based on predefining an appropriate threshold level for identifying the artifactual components. The threshold is empirically selected and is non-adaptive and context sensitive. This paper presents a new method which is based on wavelet analysis, higher order statistics, and mutual information for automatic detection of artifactual sources in ICA without requiring to train or to predefine any fixed threshold levels.

2. Methods

2.1. Independent component analysis

ICA is a statistical technique in which observed random data are linearly transformed into components that are maximally independent from each other. Let us assume that an array of sensors provides a vector of N observed signals

$$\mathbf{x}(k) = [x_1(k),\ x_2(k), \ldots, x_N(k)]^{\mathrm{T}} \tag{1}$$

that are linear mixtures of N unobservable sources,

$$\mathbf{s}(k) = [s_1(k), s_2(k), \ldots, s_N(k)]^{\mathrm{T}} \tag{2}$$

The sources are real-valued, zero-mean non-Gaussian distributed, and mutually statistically independent for each sample value k. The aim in ICA is to estimate the separating matrix, $\mathbf{W}$, such that

$$\boldsymbol{s} = \boldsymbol{W}\boldsymbol{x} \tag{3}$$

The matrix $\mathbf{W}$ defining the transformation is obtained so that the mutual information of the transformed components S_i, i.e., independent components, is minimized. Mutual information is a measure of the dependence between random variables. Several algorithms have been developed to minimize the mutual information and to find such a linear transformation. Hyvärinen [15] proposed a fast algorithm called FastICA which maximized the nongussianity. Nongussianity is here measured by the approximation of negentropy. Bell and Sejnowski [26] proposed an unsupervised learning algorithm using information maximization (Infomax) in a single-layer feedforward neural network with nonlinear outputs for blind source separation. The algorithm is effective in separating sources that have super-Gaussian distributions. However, the algorithm fails to separate sources that have negative kurtosis (e.g., uniform distribution). Lee et al. [27] extended the ability of the Infomax algorithm to perform blind source separation on linear mixtures of sources having either sub- or super-Gaussian distributions. Cardoso [28] used fourth-order cumulants to measure independence and JADE (Joint Approximate Diagonalization of Eigenmatrices) algorithm to find the separating matrix optimizing this measure. JADE is referred to a process of jointly diagonalizing a maximal set of cumulant matrices. A survey and compilation of the progress in this field is contained in [29].

2.2. ICA-based artifact suppression

One of the certain assumptions in ICA is the independency of components. Due to the fact that the nature of the ocular artifacts sources is different from that of the EEG activity, the ICA method can be used to separate the ocular artifacts and EEG brain activity into separate components. To suppress the artifacts from EEG signals using ICA, the artifactual components should be identified first. Then, the artifact-free brain signals are obtained by projecting selected non-artifactual components back onto the scalp,

Please cite this article in press as: Ghandeharion H, Erfanian A. A fully automatic ocular artifact suppression from EEG data using higher order statistics: Improved performance by wavelet analysis. Med Eng Phys (2010), doi:10.1016/j.medengphy.2010.04.010

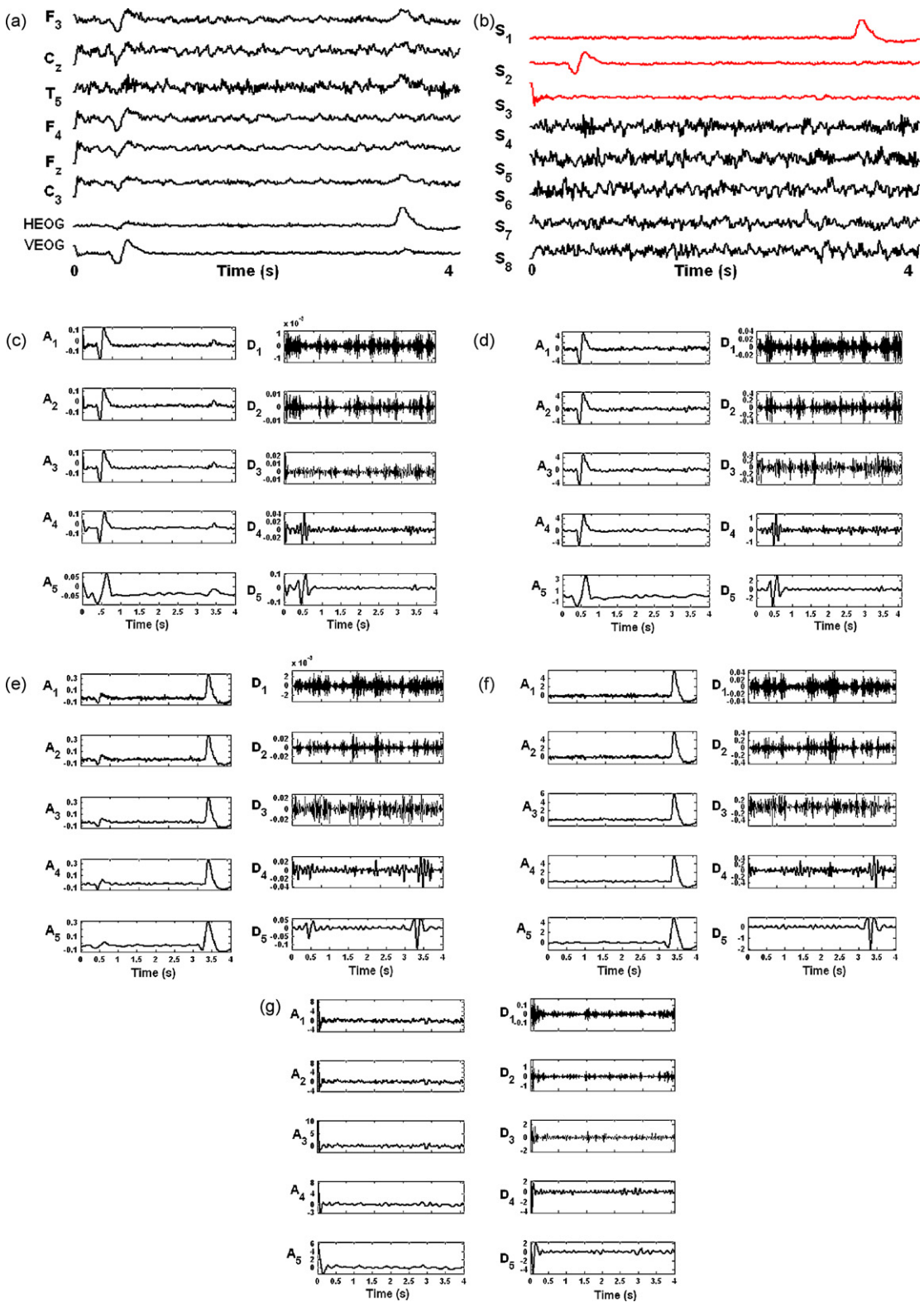

Fig. 1. A typical recorded 4-s EEG epoch (a) and corresponding independent sources extracted by extended Infomax algorithm (b). The coarse (left) and detail (right) waveforms of VEOG (c), source 2 (d), HEOG (e), source 1 (f), and source 3 (g).

$\mathbf{x}_0 = \mathbf{W}^{-1}\mathbf{s}_0$, where $\mathbf{s}_0$ is the matrix, $\mathbf{s}$, of independent components with rows representing artifactual components set to zero. To date different ICA algorithms were used to detect artifacts in EEG data and it was reported that Infomax ICA outperformed both FastICA and second-order blind inference [12,22].

2.3. Wavelet-based artifactual component detection

The wavelet transform is well-suited to analyze the irregular structures and transient phenomena in signals. By decomposing the signals into elementary building blocks that are localized both

Please cite this article in press as: Ghandeharion H, Erfanian A. A fully automatic ocular artifact suppression from EEG data using higher order statistics: Improved performance by wavelet analysis. Med Eng Phys (2010), doi:10.1016/j.medengphy.2010.04.010

Table 1
Kurtosis values of a typical 4-s recorded EOG (Fig. 1), kurtosis values of the independent components of a typical 4-s recorded EEG (Fig. 1), and kurtosis values of their coarse and detail waveforms.

	Signal	A1	A2	A3	A4	A5	D1	D2	D3	D4	D5
VEOG	11.44	11.45	11.71	11.97	13.53	9.41	0.713	1.47	3.88	10.82	13.61
HEOG	16.67	16.69	17.03	17.59	16.43	12.34	0.06	2.81	0.37	3.33	12.95
S_1	18.71	18.73	19.08	19.67	18.33	13.05	0.49	2.44	0.98	5.59	21.43
S_2	13.4	13.4	13.8	13.95	16.12	13.72	0.44	1.91	1.12	10.78	15.98
S_3	48.44	48.64	53.3	73.55	54.8	40.17	9.16	17.04	20.17	31.02	25.97
S_4	0.35	0.40	0.10	−0.03	−0.20	0.52	1.35	4.92	1.30	0.83	0.16
S_5	−0.42	−0.41	−0.43	−0.23	−0.07	0.18	0.12	1.47	1.19	0.99	0.25
S_6	−0.16	−0.15	0.01	0.44	0.82	−0.40	0.45	1.73	0.64	1.22	0.39
S_7	0.65	0.66	0.93	0.33	0.18	0.60	0.10	1.07	0.52	1.76	0.32
S_8	0.01	0.013	0.19	0.32	0.91	3.76	0.58	1.62	0.99	0.41	0.18

in space and frequency, the wavelet transform can characterize the local regularity of the signal [30]. It is important to understand the usefulness of applying wavelet analysis to distinguish EOG waves from the EEG activity. The wavelet analysis results in a set of wavelet coefficients which indicate how close the signal is to a particular basis function. Therefore, by choosing an appropriate basis function and applying the wavelet transform to the independent components, it is possible to enhance the detection of the artifactual components.

Wavelet transform has been already used for enhancing artifact suppression in EEG signals [31]. The method was based on ICA while wavelet transform was applied to the independent components and all wavelet coefficients above a certain predefined threshold were set to zero. Then, inverse wavelet transform of the coefficients was used to obtain independent components consisting neural sources only. In contrast, the current study applies wavelet transform to the independent components to enhance detection of artifactual components without using thresholding scheme.

The proposed method is based on the statistical properties of the independent components and their wavelet transform. We applied different measures for identifying the artifactual components: the kurtosis of the coarse and detail waveforms of the ICs, the correlation coefficient between ICs and the reference signals (r_V and r_H), the relative strength of each component at the vertical and horizontal EOG (c_V and c_H), and the mutual information between ICs and the reference signals.

2.3.1. Mutual information measure

The most current automatic methods for ocular artifact suppression are based on the correlation to reveal the similarity between the reference signals and the independent components [12,14,16,18,19]. In this work, we used mutual information [29] as a measure of the amount of information that the independent components contain about the EOG. Mutual information (MI) is a non-parametric measure of relevance between two random variables. Shannon's information theory provides a suitable formalism for quantifying this concept [29]. Shannon's definition of MI between two signals x and y is given as the Kullback–Leibler distance between the joint pdf $f(x,y)$ and the product of the marginal pdfs $f(x)$ and $f(y)$, i.e.,

$$I(x,y) = \int_{-\infty}^{-\infty}\int_{-\infty}^{-\infty} f(x,y)\,\log\left(\frac{f(x,y)}{f(x)f(y)}\right)\,dx\,dy \tag{4}$$

If the mutual information between two random variables is large, it means two variables are closely related. Indeed, MI is zero if and only if the two random variables are strictly independent.

One is to implement MI, its estimation poses a great difficulty as it requires the knowledge on the underlying probability density functions (pdfs) of the data and the integration on these pdfs. One of the most popular ways to estimate mutual information for low-dimensional data space is to use histograms as a pdf estimator. Histogram estimators can deliver satisfactory results under low-dimensional data spaces. Trappenberg et al. [32] have compared a number of MI estimation algorithms including a standard histogram method, an adaptive partitioning histogram method, and MI estimation based on the Gram–Charlier polynomial expansion. They have demonstrated the superior performance by the adaptive partitioning histogram method [33] in their examples.

In this work, the adaptive partitioning histogram method was used to estimate the mutual information between ICs and reference signals and ICs with maximum value were marked for possible rejection.

2.3.2. Projection strength measure

The elements of each row of the inverse matrix $\mathbf{W}^{-1}$ give the strength of a component at each of the scalp sensors. To compute the relative strength of the jth source at the vertical and horizontal EOG, the jth element of the corresponding row vector of $A = \mathbf{W}^{-1}$ is divided by its Frobenius norm as follows:

$$c_{ij} = \frac{a_{ij}}{\sqrt{\sum_k a_{ik}^2}} \times 100 \tag{5}$$

where c_{ij} is the strength percentage of source j to the ith scalp sensor and a_{ij} is the element of the mixing matrix A.

In this work, the strength of each component to the reference signals was computed and the ICs with maximum value were marked for possible rejection.

2.3.3. Correlation measure

The correlation criterion which uses second-order statistics, compare the linear relationship between the recorded EOG signals and the independent components. The similarity of independent components with the vertical and horizontal EOG is quantified by means of correlation coefficient computed as follows:

$$r_{xs} = \frac{\mathrm{Cov}(x,s)}{\sigma_x \sigma_s} \tag{6}$$

where x is the recorded reference signal, s is the independent component, σ is the standard deviation, and Cov is the covariance of the two variables x and s. The correlation coefficients between each component and reference signals were computed and ICs with maximum value were marked.

2.3.4. Kurtosis measure

Kurtosis is a fourth-order cumulant of a random variable. The kurtosis of s, denoted by kurt(s), is defined by

$$\mathrm{kurt}(s) = E(s^4) - 3[E(s^2)]^2 \tag{7}$$

where E is the statistical expectation. Kurtosis is zero for a Gaussian random variable, positive for super-Gaussian, and negative for sub-Gaussian [29]. Thus, if the kurtosis is highly positive, the activity distribution is highly peaked.

Please cite this article in press as: Ghandeharion H, Erfanian A. A fully automatic ocular artifact suppression from EEG data using higher order statistics: Improved performance by wavelet analysis. Med Eng Phys (2010), doi:10.1016/j.medengphy.2010.04.010

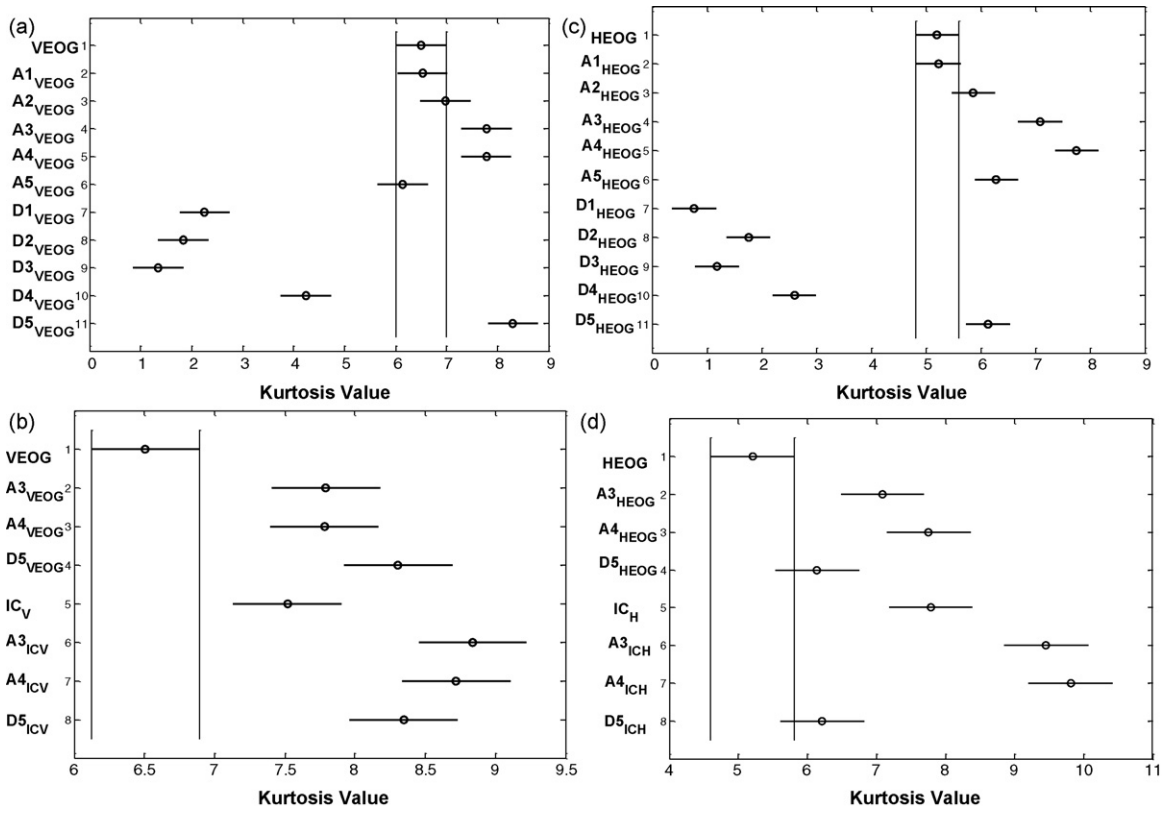

Fig. 2. Multiple comparison between kurtosis values of several pairs of variables: (a) between VEOG signal and its coarse and detail waveforms; (b) between VEOG and detail and coarse waveforms of VEOG, between VEOG and artifactual component associated with VEOG, between VEOG and detail and coarse waveforms of artifact component; (c) and (d) the same information as in (a) and (b) for HEOG.

Table 2
Average values of kurtosis of the reference signals and the coarse and detail waveforms of the references.

	Reference channel	A1	A2	A3	A4	A5	D1	D2	D3	D4	D5
Contaminated epoch											
VEOG	6.50	6.53	6.98	7.79	7.78	6.14	2.26	1.83	1.34	4.25	8.31
HEOG	5.20	5.24	5.87	7.09	7.76	6.29	0.77	1.76	1.18	2.60	6.14
Non-contaminated epoch											
VEOG	0.27	0.29	0.43	0.52	0.61	0.58	0.89	1.72	1.02	1.11	1.12
HEOG	1.64	1.67	2.08	2.96	3.56	3.76	0.80	1.88	0.93	1.14	2.72

Table 3
Mutual information between independent components of a typical recorded 4-s epoch (Fig. 1) and the reference signals.

IC	S_1	S_2	S_3	S_4	S_5	S_6	S_7	S_8
MI_{VEOG}	0.084	0.916	0.006	0.0027	0.011	0.047	0.0059	0.0037
MI_{HEOG}	0.847	0.181	0.0395	0.069	0.0009	0.0001	0.003	7.63e−6

Table 4
The measures of a typical 4-s EEG epoch (Fig. 1) contaminated by eye movements and eye-blink artifacts: kurtosis values of ICs (kurt), the relative strengths of the ICs at the two EOG channels (C_V and C_H), correlation coefficients between ICs and EOG references (r_V and r_H), mutual information between ICs and reference signals (MI_V and MI_H), and kurtosis values of coarse waveforms of the ICs.

	Kurt	r_V	r_H	MI_V	MI_H	C_V	C_H	$Kurt_{A3}$	$Kurt_{A4}$	$Kurt_{D5}$
S_1	18.71	0.17	0.97	0.08	0.85	17.11	97.02	19.67	18.33	21.43
S_2	13.4	0.95	0.19	0.92	0.18	94.97	19.87	13.95	16.12	15.98
S_3	48.44	0.26	−0.031	0.006	0.04	23.91	2.44	73.55	54.8	25.97
S_4	0.35	−0.03	−0.12	0.003	0.07	3.50	13.34	−0.026	−0.20	0.16
S_5	−0.42	0.04	0.05	0.011	0.00	1.86	2.44	−0.23	−0.07	0.25
S_6	−0.16	0.02	−0.00	0.05	0.00	2.44	0.46	0.44	0.82	0.39
S_7	0.65	−0.03	−0.00	0.01	0.00	2.53	0.08	0.33	0.18	0.32
S_8	0.01	−0.09	0.02	0.00	0.00	9.36	1.35	0.32	0.91	0.18

Please cite this article in press as: Ghandeharion H, Erfanian A. A fully automatic ocular artifact suppression from EEG data using higher order statistics: Improved performance by wavelet analysis. Med Eng Phys (2010), doi:10.1016/j.medengphy.2010.04.010

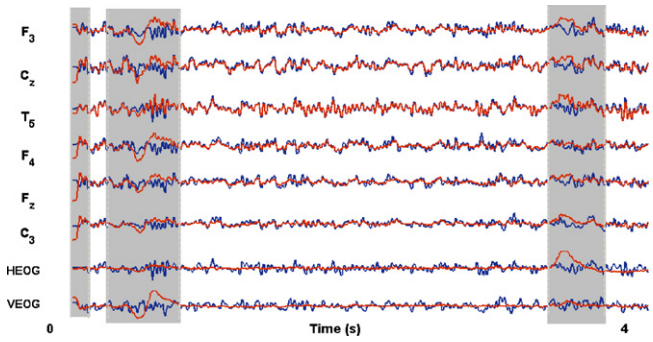

Fig. 3. A typical correction of EEG signals contaminated with ocular artifacts: recorded EEG (red line) and corrected EEG (blue line).

The kurtosis values of the detail and coarse waveforms of the components were computed and ICs with maximum values were marked for possible rejection. To compute the kurtosis, we used the built-in *kurt.m* function of Matlab (The Mathworks, R2007b).

The final decision for rejection was made based on all measures. The automatic detection system took a rejection decision for an IC when at least some of the criteria based on mutual information, correlation, projection strength, and kurtosis were satisfied.

2.4. Summary of the automatic artifact suppression procedure

The automated procedure for extracting and removing ocular components can be summarized as follows:

(1) Apply ICA to the 4-s raw EEG data, obtain mixing matrix and independent components (ICs).
(2) Apply wavelet transform to each IC.
(3) Compute the measures for each IC and its wavelet transform.
(4) For each measure, flag the IC with maximum value (for the measures of kurtosis, flag two ICs with highest values).
(5) Remove the ICs with at least four flags as the artifactual ICs.
(6) Project selected non-artifactual components back onto the scalp.
(7) Repeat steps (1)–(6) for the next 4-s raw EEG data.

2.5. Subjects and EEG data recording

The EEG data was recorded from nine healthy subjects (2 females, 7 males) by using a g.tec amplifier (g.USBamp, g.tec, Guger Technologies, Graz, Austria) and Ag/AgCl scalp electrodes from positions F3, F4, Fz, C3, Cz, and T5 according to the 10/20 system. The EOG electrodes were positioned above and below the right eye to record the vertical EOG and on the left outer canthus of the eye to record the horizontal EOG. All recording channels shared a common reference electrode at the left earlobe and a ground electrode at the right earlobe. All signals were sampled at a rate of 256 Hz and were

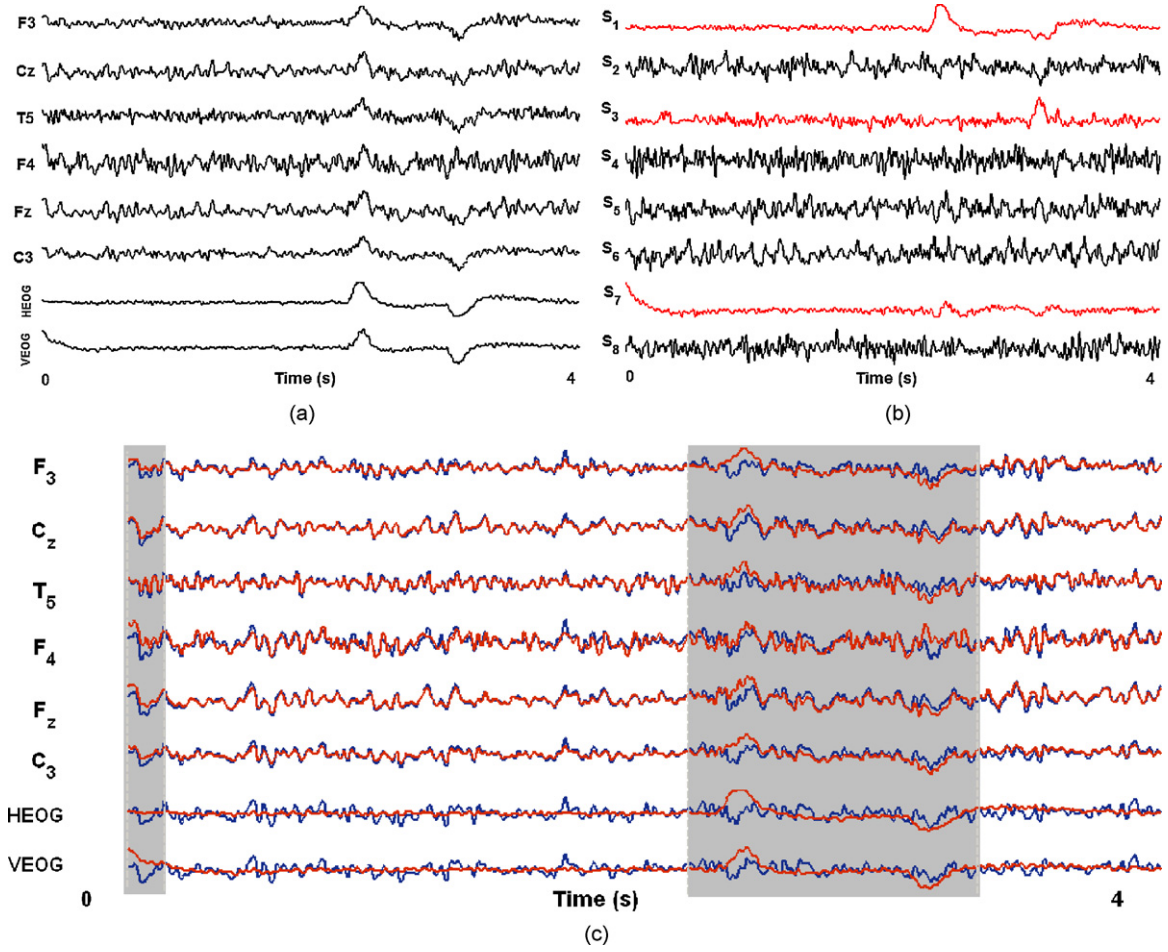

Fig. 4. (a) A portion of recorded EEG contaminated with a horizontal eye movement and a portion of eye blink. (b) Corresponding independent components. Sources 1, 3 and 7 are identified as the artifactual components by the proposed method. (c) Corrected EEG (blue line).

Please cite this article in press as: Ghandeharion H, Erfanian A. A fully automatic ocular artifact suppression from EEG data using higher order statistics: Improved performance by wavelet analysis. Med Eng Phys (2010), doi:10.1016/j.medengphy.2010.04.010

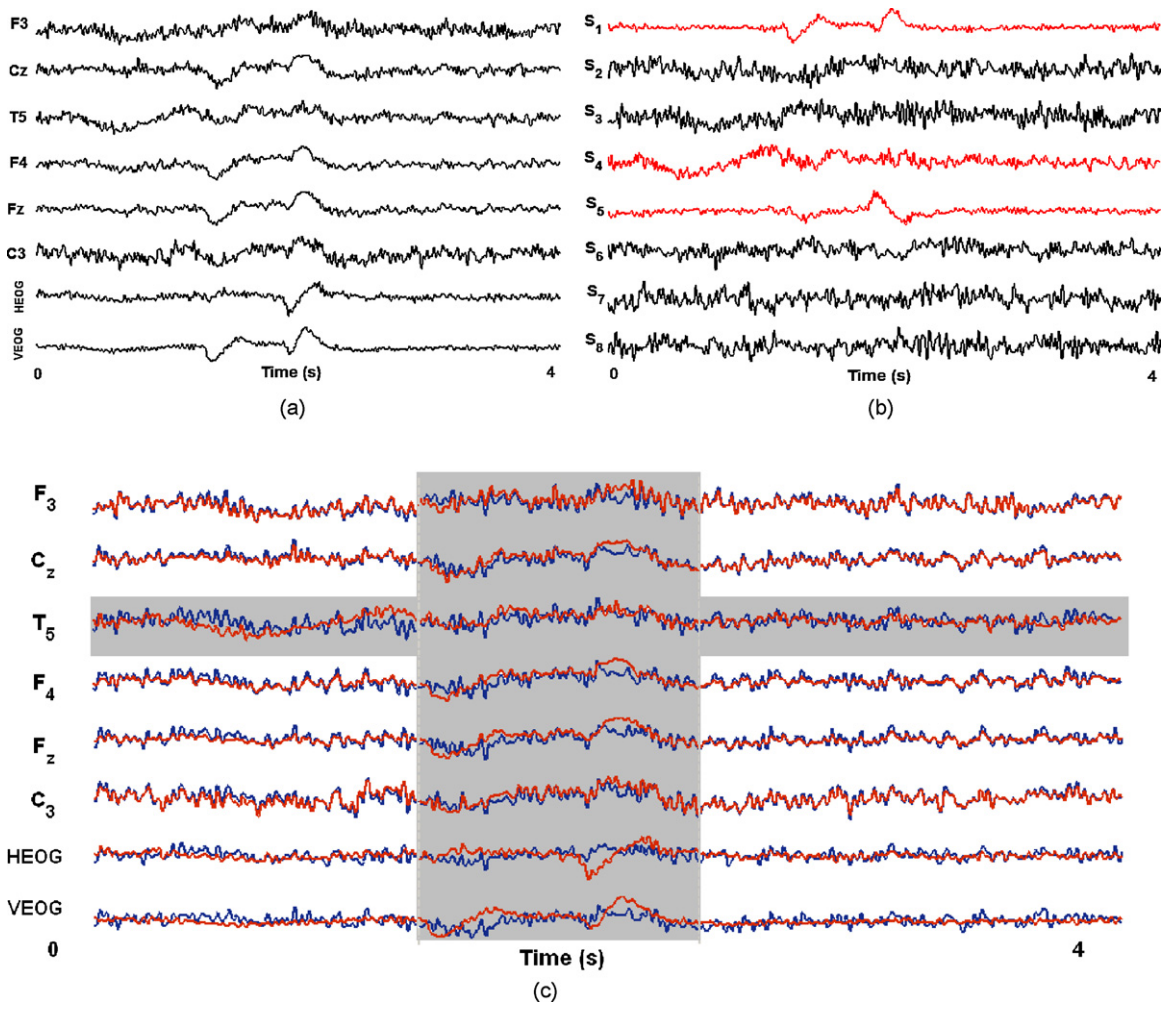

Fig. 5. (a) A portion of recorded EEG contaminated with vertical eye movements and a very slow horizontal eye movement. (b) Corresponding independent components. Sources 1, 4, and 5 are identified as the artifactual components. (c) Corrected EEG (blue line).

low-pass filtered (cutoff frequency 45 Hz). Electrode impedances were below 10 kV.

Each subject was seated in a comfortable armchair located about 1.5 m in front of a computer screen. Depending on the cue visual stimuli which was appeared on the center of screen at each 3 s, the subject was instructed to blink or not and move or not move his/her eyes horizontally or vertically. Each run of experiment lasted 60 s, while a single session of experiment consisted of between 20 and 25 runs with a 1-min break in between runs. A total of 3200 4-s EEG epochs d by two expert reviewers yielded detection of a total of non-artifactual 1469 EEG epochs and artifactual 1636 epochs. A total of 95 epochs were disregarded since it was unclear that they represented EEG activity or artifact.

3. Results

3.1. Wavelet enhanced ICA artifact detection

Fig. 1 shows a typical portion of the EEG signal contaminated by EOG, corresponding independent components, and their wavelet

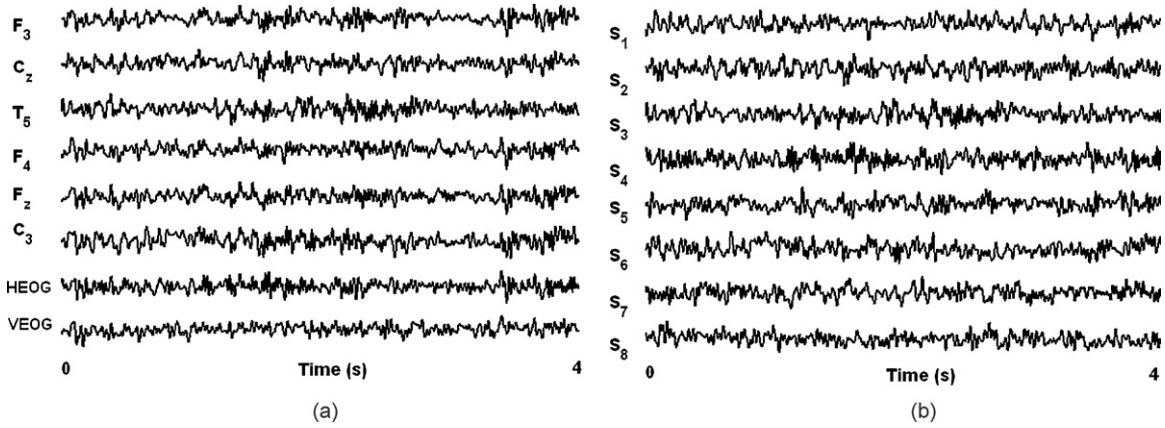

Fig. 6. (a) A typical 4-s segment of recorded artifact-free EEG. (b) Corresponding extracted independent components. No components are identified as the artifact.

Please cite this article in press as: Ghandeharion H, Erfanian A. A fully automatic ocular artifact suppression from EEG data using higher order statistics: Improved performance by wavelet analysis. Med Eng Phys (2010), doi:10.1016/j.medengphy.2010.04.010

Table 5
The measures of a typical artifact-free EEG epoch: kurtosis values of ICs (kurt), the relative strengths of the ICs at the two EOG channels (C_V and C_H), correlation coefficients between ICs and EOG references (r_V and r_H), mutual information between ICs and reference signals (MI_V and MI_H), and kurtosis values of coarse waveforms of the ICs.

	Kurt	C_H	C_V	MI_H	MI_V	r_H	r_V	$Kurt_{A3}$	$Kurt_{A4}$	$Kurt_{D5}$
S_1	0.12	0.24	0.25	0.021	0.018	24.22	24.85	0.462	0.891	0.847
S_2	−0.23	0.10	0.12	0.004	0.0042	5.91	6.40	0.045	0.521	0.066
S_3	−0.04	0.026	0.15	7e−005	0.008	2.40	15.16	0.484	0.126	1.185
S_4	−0.33	0.28	0.91	0.031	0.865	28.45	92.65	−0.349	0.134	−0.420
S_5	−0.05	0.14	0.17	0.011	0.003	7.75	9.46	−0.166	−0.464	0.508
S_6	−0.38	0.06	0.09	0.002	0.0004	5.82	9.38	−0.335	−0.034	1.143
S_7	−0.21	−0.16	−0.13	0.009	0.004	16.82	12.85	−0.238	0.05	0.493
S_8	−0.11	−0.89	−0.13	0.789	0.005	90.48	13.57	−0.288	0.461	0.316

transforms using biorthogonal 4.4 as the mother wavelet [30]. It is observed that ICA clearly separated ocular artifacts into separate components (i.e., components 1–3). Furthermore, the occurrence of ocular artifacts is detected and located by the detail signals at the levels 4 and 5. Moreover, the coarse waveforms are capable of enhancing the ocular artifacts' waveforms. To evaluate the ability of EOG detection using wavelet transform, the kurtosis is used to measure peaky activity distribution of the wavelet transform of the independent components.

Table 1 summarizes the values of kurtosis of the recorded reference signals, the wavelet transform of the references, independent components of the recorded EEG epoch, and the wavelet transform of their corresponding independent components. It is observed that the kurtosis values of the detail waveforms at the level 5 and the coarse waveforms of the EOG are higher than those of the EOG signal. The same result is obtained when the kurtosis values of the detail waveform at the level 5 and the coarse waveforms of the artifactual components are compared with the kurtosis values of the artifactual components.

A multiple comparison test, based on ANOVA [34], was used to test whether there are any differences among the mean values of kurtosis over 1636 4-s data epochs contaminated with different kinds of ocular artifacts and determine which levels of wavelet transform significantly enhance the artifact detection. The results of multiple comparison test show that the kurtosis values of detail at the level 5 and coarse waveforms of the VEOG at the levels 3 and 4 are significantly higher than the kurtosis value of the VEOG (Fig. 2(a)). Moreover, it is observed that the kurtosis values of detail and coarse waveforms of the artifactual component (i.e., $D5_{IC_V}$, $A3_{IC_V}$, $A4_{IC_V}$) are significantly higher than the kurtosis value of the artifactual component (i.e., IC_V) (Fig. 2(b)). The same results are obtained for the reference HEOG (Fig. 2(c) and (d)).

When comparing the artifactual and non-artifactual components, it is found that the kurtosis values of detail and coarse waveforms of the artifactual components (i.e., $D5_{IC}$, $A3_{IC}$, $A4_{IC}$) are significantly higher than those of non-artifactual components ($p < 0.0038$). Results of this analysis clearly indicate that the wavelet transform of independent components could significantly enhance the detection of ocular artifactual components.

Table 2 summarizes the average values of kurtosis of the recorded reference signals over 1469 4-s artifact-free epochs and over 1636 epochs contaminated with ocular artifacts. It is clearly observed that on average the kurtosis values of the detail waveforms at the level 5 and the coarse waveforms at the levels 3 and 4 are higher than those of the reference signals. The kurtosis values of the epochs contaminated by ocular artifacts are significantly higher than that of non-contaminated ones. The results presented here clearly indicate that wavelet transform can be used effectively to detect the recorded data contaminated with ocular artifacts.

Table 6
The rate of accuracy, sensitivity, and specificity for different number of criteria that need to be satisfied in order to assign a component as the artifactual component.

	Number of criteria			
	2	3	4	5
Sensitivity	63.0%	89.6%	96.9%	99.9%
Specificity	98.9%	98.6%	98.6%	94.7%
Accuracy	72.3%	93.9%	97.8%	97.0%

3.2. Mutual information

Table 3 summarizes the mutual information between each independent component and the references (i.e., recorded EOG) for a typical portion of the recorded EEG signals (Fig. 1). It is observed that MI values between the ocular artifactual components and the references are higher that those between the non-artifactual components and the references. Note that the MI values between the non-ocular artifactual component (e.g., component 3) and the reference signals are very small. The results of multiple comparison test on MI values over 3105 4-s data epochs show that the MI values between the ocular artifactual components and reference signals are significantly different from those between non-ocular components and reference signals ($p < 0.0001$).

3.3. Automatic artifact suppression

Table 4 reports the measures of a typical 4-s EEG epoch (Fig. 1) contaminated by eye movement and eye-blink artifacts. For each measurement, a component with maximum value is marked. The components with at least four markers are identified as the artifact components. It is observed that the sources 1–3 are correctly identified as the artifact components. The result of artifact correction for this EEG epoch using extended Infomax algorithm [27] is shown in Fig. 3.

The result of *N*-way ANOVA shows that the measures of ocular components are significantly different from those of non-ocular components ($p < 0.0001$). The detection method proposed here is based on the maximum values of measures. The components with at least four measures with the maximum value are assigned as the artifactual components. The result shows that the maximum values of measures associated with the EEG epochs contaminated with ocular artifacts are significantly different from those with the non-contaminated epochs ($p < 0.00038$).

Fig. 4 shows a typical EEG epoch which is contaminated with a horizontal eye movement and a portion of eye blink. The method could identify the sources 1, 3 and 7 as the artifactual components which are associated with the horizontal eye movement and eye blink. Fig. 5 shows another EEG epoch contaminated with vertical eye movements and a very slow horizontal eye movement. The procedure could identify correctly the sources 1, 4, and 5 as the artifacts associated with the vertical and horizontal eye movements. Fig. 6 shows a typical portion of recorded EEG signals with no artifact and corresponding independent components. Table 5 summarizes the measured values of this portion of EEG. It is observed that no components can be identified as the artifactual component.

Please cite this article in press as: Ghandeharion H, Erfanian A. A fully automatic ocular artifact suppression from EEG data using higher order statistics: Improved performance by wavelet analysis. Med Eng Phys (2010), doi:10.1016/j.medengphy.2010.04.010

Table 7
Results of the artifact detection using proposed method. The rows denote the actual category of the EEG epoch (as annotated by the experts), while the columns denote the classifications of the proposed method.

	Classified as artifactual epoch	Classified as non-artifactual epoch
Actual		
Artifactual epoch	1584	49
Non-artifactual epoch	20	1452

The proposed algorithm was evaluated based on reviewer's markings. The results on 3105 4-s EEG epochs indicate that the accuracy of detection is 97.8% when the decision is based on 4 measures with maximum values (Table 6). The rate of correctly identified artifactual components (i.e., sensitivity) is 96.9% while the rate of correctly identified non-artifactual components is 98.6% (i.e., specificity). The confusion matrix based on 4 measures is given in Table 7. It is observed that 20 artifact-free 4-s EEG epochs are identified incorrectly as the artifactual epoch and 49 artifactual epochs are identified as the non-artifactual. It is significant to note that the kurtosis values of the sources as well as the kurtosis values of coarse and detail waveforms of the sources at the levels 3–5 are considered as the measures for detection of artifactual sources. However, when the correlation criterion and the kurtosis values of the sources are not considered as the measures, the detection rate will be decreased from 97.8% to 95.2%.

4. Discussion and conclusions

In this paper, we have presented a fully automatic method for ocular artifact suppression employing wavelet transform and independent component analysis. In the current study, we used wavelet analysis to enhance the detection of artifactual components in an ICA-based procedure while Castellanos and Makarov [31] used the wavelet to enhance the artifact suppression. The results of current study clearly indicate that wavelet transform could significantly enhance the detection of artifactual components in an ICA-based procedure for ocular artifact suppression.

The results show that the method could identify ocular artifact components with an accuracy of 97.8%, a sensitivity of 96.9%, and a specificity of 98.6%. To the best of our knowledge, this result has not been reported before. LeVan et al. [21] who used a Bayesian classifier for identification of artifactual components in an ICA-based scheme reported that the identification of EEG components was performed with a sensitivity of 87.6% and a specificity of 70.2%.

One striking feature of the proposed method is the fully automatic identification of artifactual components without requiring calibration, predefining fixed threshold level, and pretraining. In contrast, the methods proposed by Barbati et al. [18], Joyce et al. [19], Castellanos and Makarov [31], and Romero et al. [16] are all based on thresholding scheme.

The proposed method was evaluated using only six EEG and two EOG channels. However, the method can also be applicable for more EEG channels. The effect of the number of EEG channels on the ocular artifact reduction has been already evaluated by Romero et al. [16]. Their results showed that errors in spectral parameters became higher using a configuration with few EEG electrodes. Error value obtained using BSS-based method with 19 EEG and 2 EOG channels is slightly (about 2.5%) lower than that with only 6 EEG and 2 EOG channels.

The method presented in this study needs to record EOG signals as the reference channels. However, it should be noted that although it is not needed to record EOG for applying BSS procedures, the error value not using EOG recordings is higher than those obtained when EOG channels are included in the source decomposition [16].

Acknowledgment

This work supported by Iran Neural Technology Center, Iran University of Science and Technology.

Conflict of interest

There are no conflicts of interest for the authors of this study.

References

[1] Gratton G, Coles MGH, Donchin E. A new method for off-line removal of ocular artifact. Electroenceph Clin Neurophysiol 1983;55:468–84.
[2] Woestenburg JC, Verbaten MN, Slangen JL. The removal of the eye-movement artifact from the EEG by regression analysis in the frequency domain. Biol Psychol 1983;16:127–47.
[3] Lins OG, Picton TW, Berg P, Scherg M. Ocular artifacts in recording EEG and event-related potentials. II: source dipoles and source components. Brain Topogr 1993;6:65–78.
[4] Lagerlund TD, Sharbrough FW, Busacker NE. Spatial filtering of multichannel electroencephalographic recordings through principal component analysis by singular value decomposition. J Clin Neurophysiol 1997;14:73–82.
[5] Jung T-P, Humphries C, Lee T-W, Makeig S, McKeown MJ, Iragui V, et al. Removing electroencephalographic artifacts: comparison between ICA and PCA. Neural Netw Signal Process 1998;VIII:63–72.
[6] Jung T-P, Makeig S, Humphries C, Lee T-W, Mckeown MJ, Iragui V, et al. Removing electroencephalographic artifacts by blind source separation. Psychophysiology 2000;37:163–78.
[7] Berg P, Scherg M. A multiple source approach to the correction of eye artifacts. Electroenceph Clin Neurophysiol 1994;90:229–41.
[8] Jung T-P, Humphries C, Lee T-W, Makeig S, McKeown MJ, Iragui V, et al. Extended ICA removes artifacts from electroencephalographic recordings. Adv Neural Inf Process Syst 1998;10:894–900.
[9] Ille N, Berg P, Scherg M. Artifact correction of the ongoing EEG using spatial filters based on artifact and brain signal topographies. J Clin Neurophysiol 2002;19(2):113–24.
[10] James CJ, Hesse CW. Independent component analysis for biomedical signals. Physiol Meas 2005;26:R15–39.
[11] Kierkels JJM, van Boxtel GJM, Vogten LLM. A model-based objective evaluation of eye movement correction in EEG recordings. IEEE Trans Biomed Eng 2006;53:246–53.
[12] Delorme A, Sejnowski TJ, Makeig S. Enhanced detection of artifacts in EEG data using higher-order statistics and independent component analysis. NeuroImage 2007;34:1443–9.
[13] Vigário R, Oja E. BSS and ICA in neuroinformatics: from current practices to open challenges. IEEE Rev Biomed Eng 2008;1:50–61.
[14] Wallstrom GL, Kass RE, Miller A, Cohn JF, Nathan AF. Automatic correction of ocular artifacts in the EEG: a comparison of regression-based and component-based methods. Int J Psychophysiol 2004;53:105–19.
[15] Hyvärinen A. Fast and robust fixed-point algorithms for independent component analysis. IEEE Trans Neural Netw 1999;10:626–34.
[16] Romero S, Mañanas MA, Barbanoj MJ. A comparative study of automatic techniques for ocular artifact reduction in spontaneous EEG signals based on clinical target variables: a simulation case. Comput Biol Med 2008;38:348–60.
[17] James CJ, Gibson OJ. Temporally constrained ICA: an application to artifact rejection in electromagnetic brain signal analysis. IEEE Trans Biomed Eng 2003;50:1108–16.
[18] Barbati G, Porcaro C, Zappasodi F, Rossini PM, Tecchio F. Optimization of an independent component analysis approach for artifact identification and removal in magnetoencephalographic signals. Clin Neurophysiol 2004;115:1220–32.
[19] Joyce CA, Gorodnitsky IF, Kutas M. Automatic removal of eye movement and blink artifacts from EEG data using blind component separation. Psychophysiology 2004;41:313–25.
[20] Li Y, Ma Z, Lu W, Li Y. Automatic removal of the eye blink artifact from EEG using an ICA-based template matching approach. Physiol Meas 2006;27:425–36.
[21] LeVan P, Urrestarazu E, Gotman J. A system for automatic artifact removal in ictal scalp EEG based on independent component analysis and Bayesian classification. Clin Neurophysiol 2006;117:912–27.
[22] Frank RM, Frishkoff GA. Automated protocol for evaluation of electromagnetic component separation (APECS): application of a framework for evaluating statistical methods of blink extraction from multichannel EEG. Clin Neurophysiol 2007;118:80–97.
[23] Schlögl A, Keinrath C, Zimmermann D, Scherer R, Leeb R, Pfurtscheller G. A fully automated correction method of EOG artifacts in EEG recordings. Clin Neurophysiol 2007;118:98–104.
[24] Okada Y, Jung J, Kobayashi T. An automatic identification and removal method for eye-blink artifacts in event-related magnetoencephalographic measurements. Physiol Meas 2007;28:1523–32.

Please cite this article in press as: Ghandeharion H, Erfanian A. A fully automatic ocular artifact suppression from EEG data using higher order statistics: Improved performance by wavelet analysis. Med Eng Phys (2010), doi:10.1016/j.medengphy.2010.04.010

[25] Escudero J, Hornero R, Abásolo D, Fernández A, López-Coronado M. Artifact removal in magnetoencephalogram background activity with independent component analysis. IEEE Trans Biomed Eng 2007;54:1965–73.
[26] Bell AJ, Sejnowski TJ. An information-maximization approach to blind separation and blind deconvolution. Neural Comput 1995;7:1129–59.
[27] Lee TW, Girolami M, Sejnowski TJ. Independent component analysis using an extended Infomax algorithm for mixed subgaussian and supergaussian sources. Neural Comput 1999;11:417–41.
[28] Cardoso JF. High-order contrasts for independent component analysis. Neural Comput 1999;11:157–92.
[29] Hyvärinen A, Karhunen J, Oja E. Independent component analysis. New York: John Wiley & Sons; 2001.
[30] Mallat S. A wavelet tour of signal processing. Academic Press; 1999.
[31] Castellanos NP, Makarov VA. Recovering EEG brain signals: artifact suppression with wavelet enhanced independent component analysis. J Neurosci Methods 2006;158:300–12.
[32] Trappenberg T, Ouyang J, Back A. Input variable selection: mutual information and linear mixing measures. IEEE Trans Knowl Data Eng 2006;18:37–46.
[33] Darbellay GA, Vajda I. Estimation of the information by an adaptive partitioning of the observation space. IEEE Trans Inf Theory 1999;45:1315–21.
[34] Zar JH. Biostatistical analysis. Prentice-Hall; 1999.

Please cite this article in press as: Ghandeharion H, Erfanian A. A fully automatic ocular artifact suppression from EEG data using higher order statistics: Improved performance by wavelet analysis. Med Eng Phys (2010), doi:10.1016/j.medengphy.2010.04.010